Pharmacokinetic-Pharmacodynamic Modelling of Morphine Transport Across the Blood-Brain Barrier as a Cause of the Antinociceptive Effect Delay in Rats—A Microdialysis Study

M. René Bouw,[1] Marie Gårdmark,[2] and Margareta Hammarlund-Udenaes[1,3]

Received June 11, 2000; accepted July 7, 2000

Purpose. To quantify the contribution of distributional processes across the blood-brain barrier (BBB) to the delay in antinociceptive effect of morphine in rats.

Methods. Unbound morphine concentrations were monitored in venous blood and in brain extracellular fluid (ECF) using microdialysis (MD) and in arterial blood by regular sampling. Retrodialysis by drug was used for *in vivo* calibration of the MD probes. Morphine was infused (10 or 40 mg/kg) over 10 min intravenously. Nociception, measured by the electrical stimulation vocalisation method, and blood gas status were determined.

Results. The half-life of unbound morphine in striatum was 44 min compared to 30 min in venous and arterial blood ($p < 0.05$). The BBB equilibration of morphine, expressed as the ratio of areas under the curve between striatum and venous blood, was less than unity (0.28 ± 0.09 and 0.22 ± 0.17 for 10 and 40 mg/kg), respectively, indicating active efflux of morphine across the BBB. The concentration-effect relationship exhibited a clear hysterisis with an effect delay half-life of 32 and 5 min based on arterial blood and brain ECF concentrations, respectively.

Conclusions. Eighty five percent of the effect delay was caused by morphine transport across the BBB, indicating possible involvement of rate limiting mechanisms at the receptor level or distributional phenomena for the remaining effect delay of 5 min.

KEY WORDS: morphine; nociceptive effect; electrical stimulation vocalisation method; microdialysis; retrodialysis by drug; pharmacokinetics; pharmacodynamics; modelling; blood-brain barrier transport.

INTRODUCTION

Morphine antinociception is mediated by an interaction with the μ-receptors situated at both supraspinal and spinal levels of the central nervous system (CNS). The distribution of the μ-receptors throughout the CNS is heterogeneous and species dependent (1). As the activation of the μ-receptors by morphine occurs within the CNS, the transport across the blood-brain barrier (BBB) might explain the observed delay in antinociceptive effect (2–4). Morphine penetration into the brain has been reported to be rather limited (5–8).

The use of microdialysis (MD) to study drug transport across the BBB offers the advantage of being able to determine the pharmacologically active unbound concentration closer to the site of action (9,10). The extent of drug equilibration across the BBB is expressed as the ratio of the areas under the concentration-time curve (AUC) between brain and blood. If active mechanisms are involved the transport clearance into the brain (influx) will be less than the clearance out of the brain (efflux), resulting in an AUC ratio below unity (11,12).

For CNS active drugs, the unbound concentrations in the target organ will ultimately determine the pharmacodynamic response over time. Dahlström et al. demonstrated that there is an indirect relationship between both total plasma and brain concentrations of morphine and the antinociceptive effect (3). By adapting pharmacokinetic-pharmacodynamic (PK-PD) modelling, the delay in equilibration between plasma concentration and the effect can be characterised. The half-life for the effect ($t_{1/2,keo}$) delay was later estimated to be 10 to 38 min (4,13).

This study was designed to clarify the underlying processes behind the delay in antinociceptive effect of morphine in rats. Antinociception was measured in combination with the determination of unbound concentrations in arterial blood, venous blood (MD) and brain ECF (MD) following a 10 or 40 mg/kg i.v. infusion over 10 min. The data were analysed for the involvement of active mechanisms in the transport of morphine across the BBB. A PK-PD model was developed to quantify the contribution of BBB transport to the overall delay in the onset of the antinociceptive effect.

MATERIALS AND METHODS

Chemicals

Morphine hydrochloride (10 mg/ml) was obtained from Pharmacia Upjohn AB (Stockholm, Sweden), Hypnorm® (containing fenatanyl and droperidol) from Janssen Pharmaceutica BV (Beerse, Belgium) and low molecular weight heparin from Sigma Chemicals (St Louis, USA). The perfusion solution (Ringer) for microdialysis contained 145 mM NaCl, 0.6 mM KCl, 1.0 mM $MgCl_2$, 1.2 mM $CaCl_2$ and 0.2 mM ascorbic acid in 2 mM phosphate buffer, pH 7.4. All chemicals used were of analytical grade and analytical solvents were of HPLC grade.

Animals

Male SPF Sprague Dawley rats weighing 280–335 g were used (Møllegård, Denmark). The animals were acclimatised in groups of four per cage and maintained in a controlled environment (22 ± 1 °C) with a normal light-dark cycle. They were allowed to adapt for at least one week prior to surgery and had access to food (ALAB, Sollentuna, Sweden) and tap water *ad libitum.* The study was approved by the Animal Ethics Committee of Uppsala University (C328/95).

Surgical Procedure

The femoral artery and vein were cannulated under Hypnorm® anesthesia (0.2 mg/kg, i.m.) using PE-10 connected to PE-50 tubing for blood sampling and drug administration. A

[1] Division of Biopharmaceutics and Pharmacokinetics, Department of Pharmacy, University of Uppsala, Uppsala, Sweden.
[2] Medical Products Agency, Uppsala, Sweden.
[3] To whom correspondence should be addressed at Division of Biopharmaceutics and Pharmacokinetics, University of Uppsala, Box 580, S-751 23 Uppsala, Sweden. (e-mail: Margareta.Hammarlund-Udenaes@biof.uu.se)

0724-8741/00/1000-1220$18.00/0

15 cm piece of PE-50 tubing, looped subcutaneously distal to the posterior surface of the neck, was used to adjust the perfusion solution to body temperature before it entered the striatal probe. For blood microdialysis, a CMA/20 (CMA, Stockholm, Sweden) probe with a 10 mm membrane length was inserted into the right jugular vein and anchored to the pectoral muscle. During insertion, the probe was perfused with a 0.1 % low molecular weight heparin solution to minimise the incidence of clotting. A guide cannula with dummy probe was stereotaxically placed in striatum of the right brain hemisphere (anterior: 0.8 mm and lateral: 2.7 mm with bregma as a reference and 3.8 mm ventral to the brain surface). Two pieces of steel suture were placed intracutaneously, 1 and 3 cm distal from the root of the tail. Protruding ends of all cannulae and probe tubings were tunnelled subcutaneously and externalised on the posterior surface of the neck. The rats were placed in a CMA/120 system for freely moving animals and were allowed to recover for 24 hours.

In Vivo Calibration of the MD Probes

On the day of the microdialysis experiment a 3 mm CMA/12 probe (CMA, Stockholm, Sweden) was inserted into the guide cannula. Both probes were perfused with blank Ringer's solution at a flow rate of 2 μl/min. Microdialysate fractions were collected automatically using a CMA/140 Microfraction collector (CMA, Stockholm, Sweden) every 10 min unless otherwise stated. After a stabilisation period of one hour, the *in vivo* recovery was estimated using retrodialysis by drug (14). For one hour, MD probes were perfused with a morphine solution containing 100 ng/ml (blood) or 200 ng/ml (striatum). Unbound concentrations of morphine were calculated from the dialysate concentration of morphine adjusted for the *in vivo* recovery value. After the retrodialysis period, the probes were perfused for one hour with blank perfusion solution.

Experimental Design for In Vivo MD

The rats were randomly assigned into two groups receiving an i.v. infusion of morphine hydrochloride over 10 min. Group 1 (n = 9) was administered a dose of 10 mg/kg, while Group 2 (n = 9) received a 40 mg/kg dose. Microdialysates were collected over a period of 190 min into pre-weighed vials. Samples were taken at 5 min intervals during the infusion, at 10 min intervals over the following hour and at 15 min intervals over the remaining 2 hours. Arterial blood samples (100–150 μl) were collected in heparinized vials at 0, 8, 20, 70, 130 and 190 min. After collection, samples were centrifuged at 5000 r.p.m. for 5 min, and plasma was harvested and frozen at –20 °C until analysis.

Measurement of the Antinociceptive Effect

Antinociception was measured using a GRASS S88 according to the electrical stimulation vocalisation method (15). An electrical stimulus was applied to the two electrodes implanted in the tail of the rat and the vocalisation response was recorded as the endpoint, i.e. the pain threshold. The baseline value of the pain threshold was estimated three times at 15 min intervals before the start of the experiment. Antinociception was recorded at the end of the blank, retrodialysis and washout period and at 5, 10, 15, 20, 30, 40, and 55 min after the start of the infusion and thereafter every 15 min up to 190 min.

Monitoring of Blood Gas Status

The blood gas status of the rats was monitored by injection of a 50 μl arterial blood sample into an AVL Compact II blood gas analyser (AVL Medical Nordic, Stockholm, Sweden) to determine the arterial pO_2, pCO_2, O_2 saturation and pH. During the experiment the blood gas status was monitored just before antinociception was measured, except for 145 and 175 min.

Analysis of Morphine

Concentrations of morphine in microdialysates and plasma were determined by HPLC. The chromatographic equipment consisted of an auto injector (Triathlon, Spark Holland, The Netherlands), a pump (ESA 580, ESA Inc., USA), a reversed phase column (Nucleosil C-18, 5μm, 150 × 4.6 mm i.d., Chrompack, Sweden), an electrochemical detector (Coulochem II, ESA Inc., USA) and an integrator (Shimadzu CR-5A, Shimadzu Europe, Sweden). An aliquot of 17 μl was used to determine morphine using electrochemical detection (Detector 1, 0 mV; Detector 2, +450 mV; Guard cell, + 500 mV). The mobile phase consisted of 550 ml 0.01 M phosphate buffer, pH 2.1, containing 0.2 mM dodecyl sulphate and 450 ml methanol, and was delivered at a flow rate of 1.0 ml/min. The limit of quantification in the MD samples was 3 ng/ml (10.5 nM), with a coefficient of variation (CV) of 5.9 %.

Morphine concentrations in plasma were determined with the chromatographic system as described above, except that the potential of detector 1 was increased from 0 to 350 mV. The mobile phase was changed to 680 ml 0.01 M phosphate buffer, pH 2.1, containing 0.2 mM dodecyl sulphate, 320 ml methanol and 25 ml tetrahydrofuran. Pre-treatment of the plasma samples (100 μl) was performed as described earlier (4). The limit of quantification for morphine was 6 ng/ml (21 nM), with a CV of 5.2 %. The absolute extraction recovery of morphine from plasma samples was 100 ± 3 %.

Pharmacokinetic Analysis

The pharmacokinetic parameters of unbound morphine in arterial plasma were estimated by non-compartmental analysis according to standard procedures (4). The unbound arterial concentrations of morphine were estimated using a protein binding of 20 % (16). The extent of BBB equilibration of morphine was expressed as the ratio in area under the unbound concentration time curves (AUC_u) between striatum and venous blood.

Pharmacokinetic-Pharmacodynamic Modelling

The unbound concentration and effect data were analysed by nonlinear mixed effect modelling using the program NONMEM (version VI) and the first order method (17). Differences in unbound morphine concentrations in blood and striatum between individual rats are accounted for by this modelling procedure. Population mean parameters were assessed, as well as interindividual and residual variability. An exponential variance model was used to describe the intera-

nimal variability for all parameters. The residual errors were characterised by a proportional error model. Graphic analysis of the residuals and predictions, implemented in Xpose 2.0 (18) and a decrease in the objective function (–2log likelihood) provided by NONMEM, were used to discriminate between different models. However for studies like this, with rich data, the change in objective function value should exceed the critical value of 3.84, as set for model discrimination in sparse data analysis (17).

The combined data from all rats were fitted simultaneously. A two-compartment model expressed in terms of clearance (CL) and volume (V1–2) best described the unbound arterial concentration time profiles. The individual estimates of the parameters, derived by Bayesian analysis, were used as a forcing function during the next step of the modelling. The following models were built to describe the unbound concentration effect relationship of morphine related to different tissue concentrations. Both the link model and the indirect response model were tested. The link model performed better with these data, and is presented below.

Model 1—Unbound Arterial Concentrations as the Input Function (Fig. 1A)

The time course of the effect site concentration is described by the rate constant, k_{e0}, out of the effect compartment (19). Different pharmacodynamic models (i.e., linear, E_{max} and sigmoid E_{max}) were tested, and the sigmoid E_{max} model best described the relationship between the arterial plasma concentration of morphine and the antinociceptive effect of morphine (E), according to:

$$E = E_0 + \frac{E_{max} \times C_e^{\,n}}{EC_{u,50}^{\,n} + C_e^{\,n}} \quad (1)$$

where C_e is the effect site concentration, E_0 is the baseline effect when no morphine is present, $EC_{u,50}$ is the unbound plasma steady state concentration that corresponds to 50% of the maximal effect (E_{max}) and n is a constant, expressing the sigmoidicity of the curve.

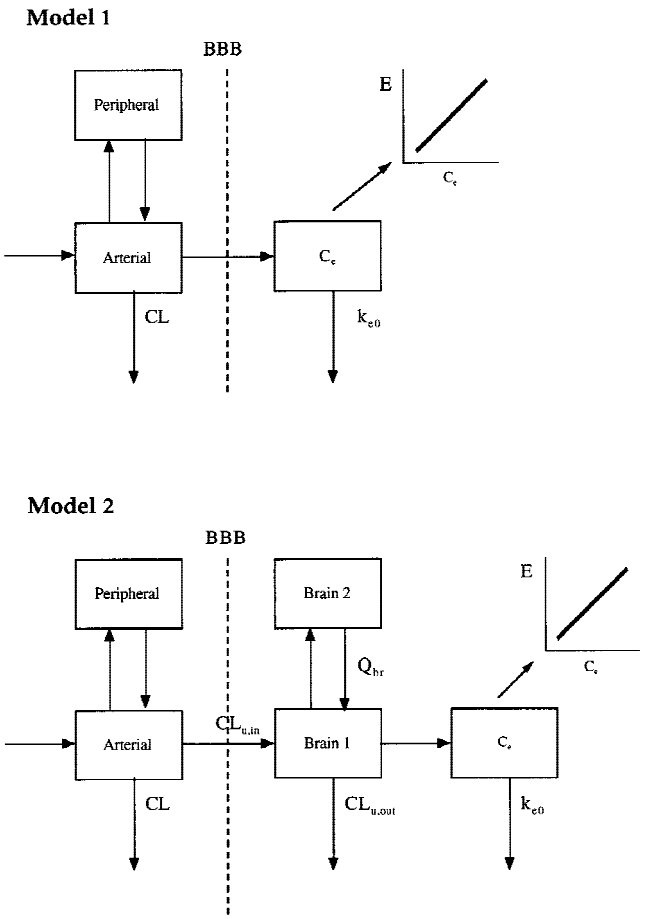

Fig. 1. Pharmacokinetic-pharmacodynamic models of morphine. A. Model 1 with arterial concentrations as the driving force for the nociceptive response of morphine. B. Model 2 with brain ECF concentrations as the driving force.

Model 2—Brain ECF Concentrations as the Input Function (Fig. 1B)

Firstly, the individual arterial plasma parameters from the initial step were used as a forcing function to describe the ECF concentration time curves of morphine in the brain. A two-compartment model was necessary to obtain an adequate description of the unbound concentration-time profiles in brain. The brain compartments were connected by an intercompartmental clearance Q_{br} and were defined as brain 1 and brain 2, respectively. Mass transfer from the brain to the arterial compartment was ignored as the amount of drug in the brain is very small compared to the amount of drug in the rest of the body (Fig. 1 B).

The unbound apparent volume of distribution ($V_{u,app}$) in the brain ECF, necessary to parameterise the kinetic model in terms of clearance and unbound concentrations, was described by:

$$V_{u,app} = \frac{(A_{br} - V_{bl} \times C_{bl})}{C_{u,br1}} \quad (2)$$

where A_{br} is the total amount of morphine per gram of brain (g-brain), V_{bl} is the blood volume per g-brain, C_{bl} is the arterial concentration and $C_{u,br1}$ is the unbound ECF concentration of morphine in brain. According to the literature the blood to plasma ratio of morphine at a hematocrit of 44 % is 1.27 (20) and V_{bl} is 15 μl/g-brain (7). Based on steady-state estimates of A_{br}, C_{bl} and $C_{u,br1}$ in mice (21), a $V_{u,app}$ of 1.3 ml/g-brain was obtained and used as a fixed parameter in the regression analysis. The unbound volume of distribution in brain compartment 2 ($V_{u,br2}$) is equal to ($V_{u,app}$-$V_{u,br1}$). The distribution of morphine in the brain ECF is given by:

$$V_{u,br1} \times \frac{dC_{u,br1}}{dt} = CL_{in} \times C_{u,art} + Q_{br} \times C_{u,br2} - (CL_{out} + Q_{br}) \times C_{u,br1} \quad (3)$$

where $C_{u,art}$ is the unbound morphine concentration in arterial plasma, $C_{u,br1}$ and $C_{u,br2}$ are the unbound morphine concentrations in the respective brain compartments, CL_{in} is the influx clearance into the brain, CL_{out} is the efflux clearance out of the brain, Q_{br} is the intercompartmental clearance and $V_{u,br1}$ is the estimated unbound volume of distribution in brain compartment 1. As seen with Model 1 the sigmoid E_{max} model best described the relationship between the brain ECF concentrations of morphine and the antinociceptive effect. Finally, in order to clarify whether the delay found in Model 2 was significant from zero time, the antinociceptive

Table 1. Pharmacokinetic Parameter Estimates Obtained After a 10 min Infusion of 10 or 40 mg/kg Morphine in Rats (Means (CV))

Dose	AUC ratio[a]	Half-life (min) Arterial blood	Venous blood	Striatum	CL_u (ml/min/kg)
10 mg/kg	0.28 (32)	34.1 (30)	30.2 (27)	44.3 (25)[b]	103.5 (28)
40 mg/kg	0.22 (77)	28.6 (11)	29.1 (14)	42.1 (13)[b]	69.9 (16)[c]

[a] Expressed as the ratio $AUC_{u,striatum}$ and $AUC_{u,venous\ blood}$.
[b] Significantly different from both venous and arterial blood ($p < 0.05$).
[c] Significant difference between dose groups ($p < 0.05$).

effect was also directly related to the ECF concentration of morphine without an effect compartment.

Statistics

All pharmacokinetic data are reported as means with the coefficient of variation in parentheses (%). Any significant differences in $t_{1/2}$, AUC ratio and CL_u between Groups 1 and 2 were evaluated by unpaired t-test ($p < 0.05$).

RESULTS

The *in vivo* recovery estimated from retrodialysis by drug was 8.4 ± 3.8 % (range: 4.3–21.8 between probes) in striatum and 40.9 ± 14.6 % (range: 20.5–64.5 between probes) in blood.

The equilibration of morphine across the BBB, expressed as the AUC ratio between brain and venous blood, was 0.28 ± 0.09 for Group 1 and 0.22 ± 0.17 for Group 2, indicating the involvement of active mechanisms in morphine transport across the BBB (Table 1). The influx clearance (CL_{in}) and efflux clearance (CL_{out}) were estimated using Model 2 as 14 ± 0.6 μl/min*g-brain and 40 ± 1.4 μl/min*g-brain, respectively. This resulted in a Cl_{in}/Cl_{out} ratio of 0.35, which was in good agreement with the AUC ratio of morphine in brain to that in arterial blood.

The half-life in brain of 44 min was significantly longer ($p < 0.05$) than that of 30 min in arterial and venous blood (Table 1, Fig. 2). No significant differences in half-lives were found between the two groups. However, the unbound clearance of morphine was significantly lower after the 40 mg/kg dose than after the 10 mg/kg dose, as reported from earlier studies (4,22).

The perfusion of the microdialysis probes during the blank period, the calibration period and the washout period

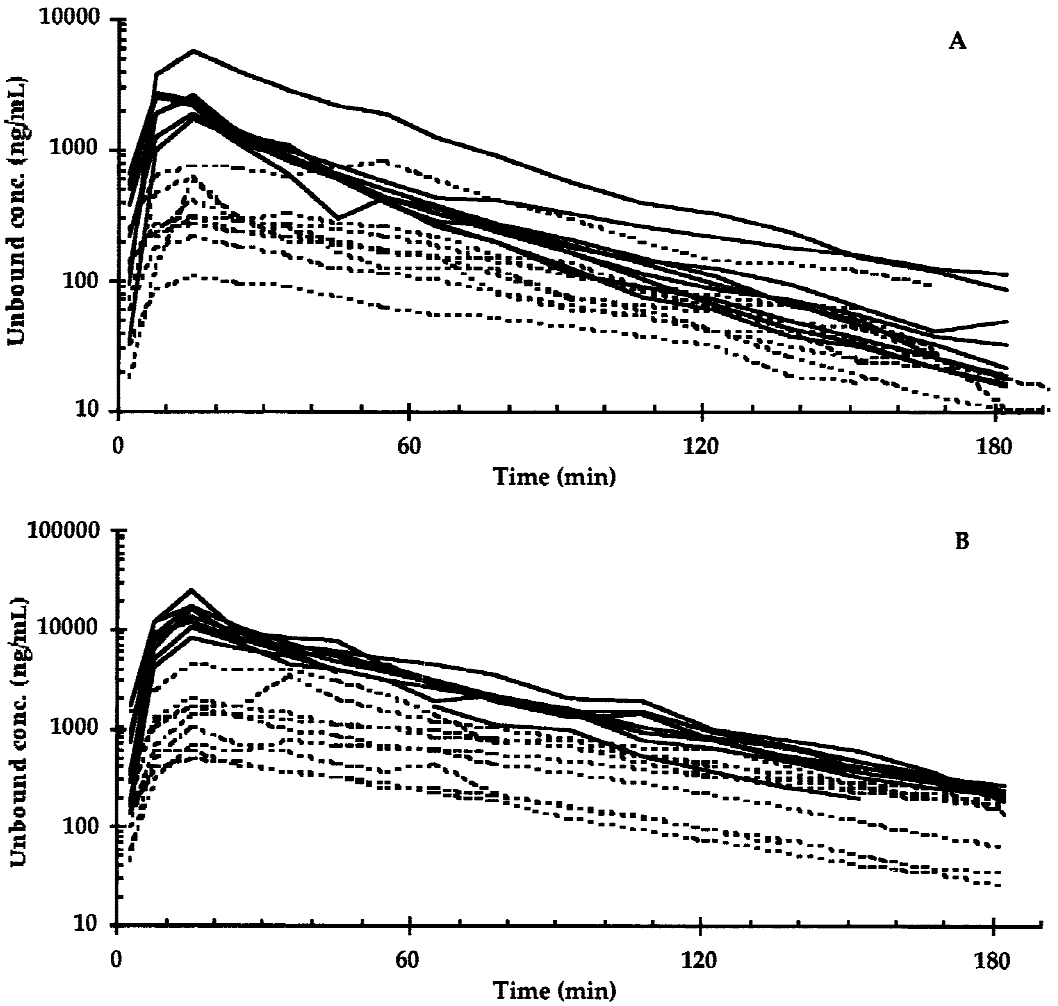

Fig. 2. Individual unbound morphine concentrations in venous blood (solid lines) and in brain ECF (dashed lines) upon administration of a 10 min infusion of 10 mg/kg (A) or 40 mg/kg (B).

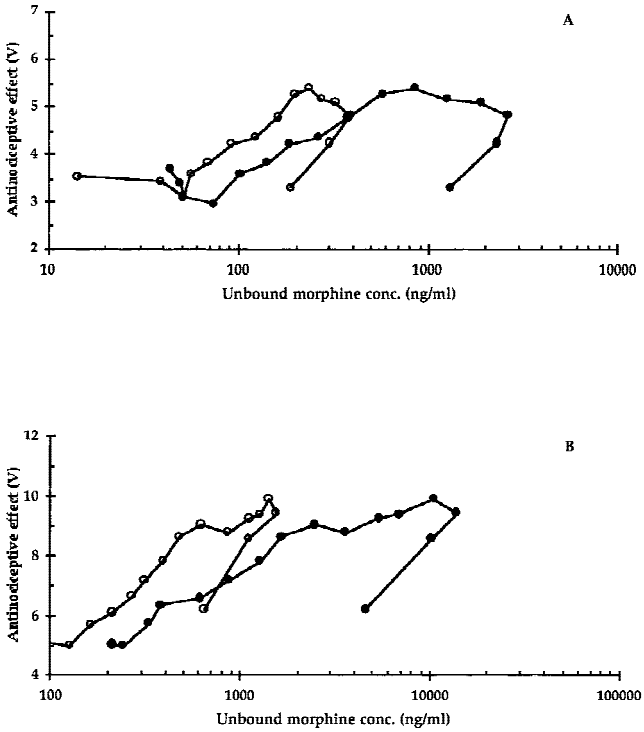

Fig. 3. Averaged concentration-antinociceptive effect relationship of morphine in venous blood (filled circles) and in brain ECF (open circles) upon administration of a 10 min infusion of 10 mg/kg (panel A) or 40 mg/kg (panel B).

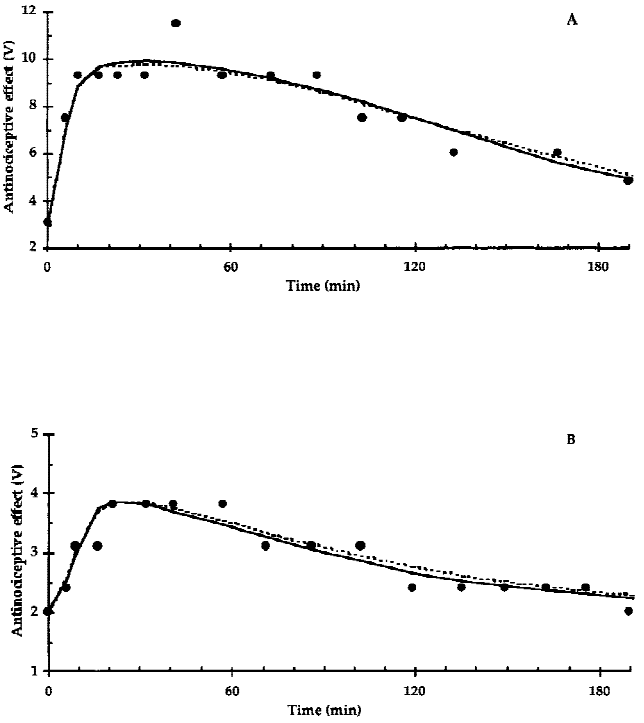

Fig. 4. The observed (filled circles) and predicted antinociceptive effect over time in relation to morphine concentrations in arterial blood (solid line) or in brain ECF (dashed line) upon administration of a 10 min infusion of 40 mg/kg (panel A) or 10 mg/kg (panel B) to two representative rats.

had no influence on the baseline nociceptive response. For Group 1 the antinociceptive effect increased from a baseline of 2.4 V to a maximum of 5.4 V (225 %), while for Group 2 an increase from 2.9 V to 9.9 V (341 %) was observed. The maximal peak effect was reached at 44 min for Group 1 and at 22 min for Group 2.

As expected, a pronounced hysteresis was observed between venous morphine concentrations and the antinociceptive effect (Fig. 3). There was still a delay when brain ECF concentrations of morphine were related to the antinociceptive effect. For both Models 1 and 2 the sigmoid Emax model performed best of all the models tested in describing the antinociceptive effect of morphine (Fig. 4). In both groups, the hysteresis was successfully minimised using Models 1 and 2 (Fig. 5). The overall effect delay half-life for morphine in Model 1 was estimated to 32 min, while a remaining effect delay half-life of 5 min was observed in Model 2 (Table 2). Similar E_{max} and E_0 values were estimated for both models, although the interanimal variability was lowest for Model 2. Using a direct relationship between brain ECF concentration and antinociceptive effect it was possible to show that the 5 min effect delay from Model 2 was significantly different from zero. This was demonstrated by a large elevation in the objective function value compared to the link model (Table 2).

The 10 mg/kg dose of morphine had only a minor influence on the respiratory parameters (pH, pO_2 and pCO_2). The 40 mg/kg dose of morphine resulted in an average increase in pCO_2 from 5.3 ± 1.7 to 8.5 ± 1.6 kPa. This increase in pCO_2 was counterbalanced by a pronounced decrease in pH from 7.41 ± 0.04 to 7.21 ± 0.12 and in pO_2 from 11.4 ± 0.71 to 5.4 ± 0.63 kPa, respectively. The respiratory parameters returned to baseline values after 70 min in Group 1, while the baseline values for all except the pO_2 level were attained after 150 min in Group 2. Although average AUC ratios did not differ between the two groups, rats with a lower minimal arterial pH also had a lower striatum: venous blood AUC ratio for morphine concentration (Fig. 6). The relationship between the AUC ratio and the minimal arterial pH was described by an exponential function using regression analysis ($r^2 = 0.57$, $p < 0.05$).

DISCUSSION

In this study we have quantified the contribution of distributional processes across the BBB to the overall delay in effect of morphine. A clear effect delay half-life of 32 min was observed for the antinociception related to arterial concentrations. A remaining effect delay of 5 min was found in relation to morphine concentrations in brain.

The observed effect delay half-life of 32 min is in good agreement with earlier reported values of 25 min (22) and 38 min (4). In contrast, studies using the tail flick method have shown a shorter delay in onset of the effect ranging from 3 to 14 min (23–25). A possible explanation for the different findings in effect delay might be that the tail flick method is a spinally mediated response, whereas the electrical stimulation vocalisation method reflects an integrated response at higher levels in the CNS. In a study comparing different nociceptive tests, Gårdmark and colleagues showed that although the tail flick method was more sensitive to morphine nociception than the electrical stimulation vocalisation method, it was also more variable in outcome. With the tail flick method, several ob-

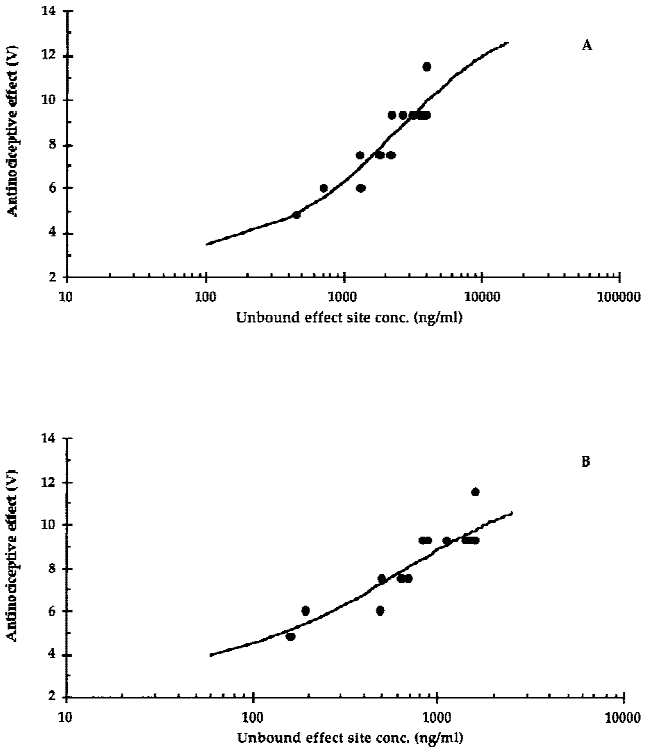

Fig. 5. The antinociceptive effect (filled circles) versus unbound effect-site concentration of morphine in relation to arterial blood (panel A) or brain (panel B) in a representative rat (see Fig. 4 A). The solid line represents the individual fit to the individual pharmacodynamic model.

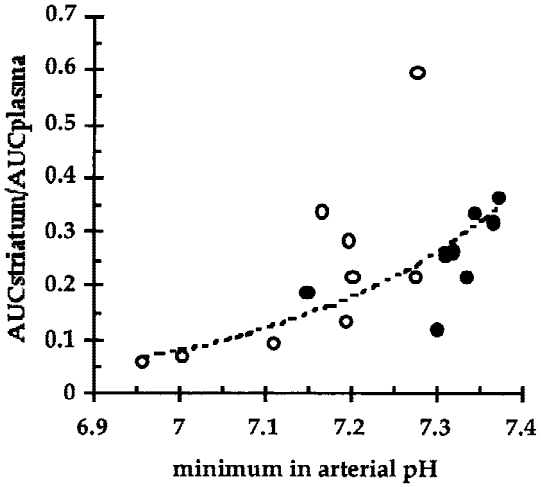

Fig. 6. The extent of transport across the BBB, expressed as the ratio AUCstriatum:AUCplasma versus minimal arterial pH in individual rats after a 10 mg/kg (filled circles) or 40 mg/kg dose (open circles) of morphine over 10 min. Dotted line represents the exponential correlation between AUC ratio and pH ($r^2 = 0.57$, $p < 0.05$).

servations (59 %) reached the cut-off latency point at subcutaneous doses of 5 mg/kg, which made pharmacodynamic analysis of the data difficult as the cut-off latency is not equal to the maximal effect (E_{max}) of the drug (26).

In an early report by Dahlström et al., it was shown that total brain concentrations of morphine were not directly related to the antinociceptive effect (3). MD allows the origin of the observed delay to be revealed, as it is capable of monitoring extracellular morphine concentrations closer to the site of action. Data from our sequential model suggested that distributional processes across the BBB account for 27 min (85%) of the total effect delay. For the remaining effect delay of 5 min at the CNS level we can only speculate that either rate limiting mechanisms at the receptor level or further distribution phenomena within the brain are contributing.

The equilibration of morphine across the BBB was expressed as the unbound AUC ratio between brain and venous blood. The ratios of 0.22 and 0.28, for the 10 and 40 mg/kg doses, respectively, indicates an involvement of active efflux mechanisms at the BBB. This is in agreement with a 3-fold higher unbound extracellular concentration of morphine in the brain in P-gp knock-out mice than in wild-type mice (21). Letrent et al. showed that P-gp inhibition significantly increased the brain distribution of unbound morphine in rats from 0.47 to 1.21 (27). In contrast, Stain et al. showed an unbound AUC ratio of 1.2 in rats (28).

MD can be used to monitor the unbound concentrations

Table 2. Pharmacodynamic Parameter Estimates (Mean (CV%)) Obtained by Population Analysis of Intravenous Morphine 10 or 40 mg/kg in Rats Using Models 1 and 2

	Model 1		Model 2			
	Link model		Link model		Direct model	
	Parameter Estimate	Inter-animal variability[a]	Parameter estimate	Inter-animal variability[a]	Parameter estimate	Inter-animal variability[a]
k_{eo} (min^{-1})	0.022 (11)	48	0.143[d] (18)	64	NE	NE
$t_{1/2,keo}$ (min)[b]	32.2	NE	4.9	NE	NE	NE
E_o (V)	2.7 (4)	24	2.7 (5)	16	2.6 (5)	37
Emax (V)	10.1 (13)	70	10.9 (10)	17	10.5 (23)	110
$EC_{u,50}$ (ng/ml)	1740 (28)	79	770[c] (34)	73	827 (72)	37
n	0.93 (15)	76	0.68[c] (11)	21	0.61 (15)	140
Obj. val.	74		96		229	

[a] Coefficient of variation (%).
[b] Derived parameter ($t_{1/2} = \ln 2/k_{eo}$).
[c] $p < 0.05$, post-hoc paired t-test between arterial blood (Model 1) and brain ECF (Model 2).

of drugs in the brain and thence determine the influx and efflux permeability of the BBB to drugs (11,29). The influx clearance of 14 μl/min*g-brain found in this study exceeded previously reported values for the permeability surface area product (PS) of 3.5–8.0 μl/min*g-brain (7,8). The PS values were determined using the intravenous injection technique where efflux from brain to blood during the one hour study period was assumed to be negligible. Our results show that there is considerable efflux from brain to blood and therefore the permeability of the BBB to morphine is likely to be underestimated by the intravenous injection technique if measurements are taken over such a long period.

The half-life of morphine in brain was longer than in blood. The difference demonstrates that morphine elimination from the CNS is rate-limited by redistribution of the drug from brain tissue rather than being governed by the pharmacokinetics of morphine in blood. Therefore, a two compartment model was necessary in order to describe the distribution of morphine in the brain.

There was a large variation in AUC ratio after administration of the 40 mg/kg dose, which correlated well with individual respiratory response. The correlation between the AUC ratio and the minimal arterial pH in this study suggests that respiratory acidosis might decrease the transport of morphine across the BBB (Fig. 5). This observation is consistent with the fact that, since the pKa value of morphine is 7.93, there is less unionised morphine available for transport across the BBB at lower pH.

In humans and most rodents, morphine is metabolised by glucuronidation in the liver. The lack of formation of morphine-6-glucuronide (30) and the fact that morphine-3-glucuronide antagonises the antinociceptive effect only to a minor extent (24,31,32) make the rat an ideal model for the study of the genuine antinociceptive effect of morphine itself, without confounding metabolite effects. On the other hand, long term exposure to morphine does affect its pharmacological activity; the antinociceptive effect is decreased as tolerance develops (4,23). Our group has studied the development of acute tolerance to morphine. In one of the studies, rats received three different morphine infusion regimens aiming at the same target plasma concentration. The tolerance development was estimated with a half-life of 48 min (4). These results showed that there was a negligible tolerance development during the 10 min infusion. Therefore tolerance was not included in the PK-PD model in the present paper.

In summary, this study confirms that morphine is actively effluxed at the BBB. Once inside the CNS, morphine elimination from the brain is rate-limited by redistribution within the brain tissue, leading to a longer half-life in the brain than in blood. The simultaneous determination of the unbound concentrations of morphine in blood and in the CNS enabled us to develop a sequential PK-PD model to characterise the origin of the effect delay. The transport of morphine across the BBB could explain up to 85 % of the overall delay in antinociceptive effect, indicating a possible involvement of pharmacodynamic factors in the remaining effect delay of 5 min.

ACKNOWLEDGMENTS

The authors gratefully acknowledge the laboratory assistance of Britt Jansson for the morphine plasma analysis. The study was supported by grants from the Swedish Medical Research Council (Project no. 11558).

REFERENCES

1. A. Mansour and S. J. Watson. Anatomical distribution of opioid receptors in mammalians: An overview. In H. Akil and E.J. Simon (eds), *Opioids I,* Springer-Verlag, Berlin, 1993, pp. 79–102.
2. B. E. Dahlström and L. K. Paalzow. Pharmacokinetics of morphine in plasma and discrete areas of the rat brain. *J. Pharmacokinet. Biopharm.* **3**:293–302 (1975).
3. B. E. Dahlström, L. K. Paalzow, G. Segre, and A. J. Ågren. Relation between morphine pharmacokinetics and analgesia. *J.Pharmacokinet. Biopharm.* **6**:41–53 (1978).
4. M. Gårdmark, M. Ekblom, R. Bouw, and M. Hammarlund-Udenaes. Quantification of effect delay and acute tolerance development to morphine in the rat. *J. Pharmacol. Exp. Ther.* **267**: 1061–1067 (1993).
5. W. H. Oldendorf, S. Hyman, L. Braun, and S. Z. Oldendorf. Blood-brain barrier: Penetration of morphine, codeine, heroin, and methadone after carotid injection. *Science* **178**:984–986 (1972).
6. T. A. Aasmundstad, J. Morland, and R. E. Paulsen. Distribution of morphine 6-glucuronide and morphine across the blood-brain barrier in awake, freely moving rats investigated by in vivo microdialysis sampling. *J. Pharmacol. Exp. Ther.* **275**:435–441 (1995).
7. U. Bickel, O. P. Schumacher, Y. S. Kang, and K. Voigt. Poor permeability of morphine 3-glucuronide and morphine 6-glucuronide through the blood-brain barrier in the rat. *J Pharmacol Exp Ther.* **278**:107–113 (1996).
8. D. Wu, Y. S. Kang, U. Bickel, and W. M. Pardridge. Blood-brain barrier permeability to morphine-6-glucuronide is markedly reduced compared with morphine. *Drug Metab Dispos.* **25**:768–771 (1997).
9. E. C. M. de Lange, M. Danhof, A. G. de Boer, and D. D. Breimer. Methodological considerations of intracerebral microdialysis in pharmacokinetic studies on drug transport across the blood-brain barrier. *Brain. Res. Rev.* **25**:27–49 (1997).
10. W. F. Elmquist and R. J. Sawchuk. Application of microdialysis in pharmacokinetic studies. *Pharm. Res.* **14**:267–288 (1997).
11. Y. Wang and D. F. Welty. The simultaneous estimation of the influx and efflux blood-brain barrier permeabilities of gabapentin using a microdialysis-pharmacokinetic approach. *Pharm Res.* **13**: 398–403 (1996).
12. M. Hammarlund-Udenaes, L. K. Paalzow, and E. C. M. de Lange. Drug equilibration across the blood-brain barrier—Pharmacokinetic considerations based on the microdialysis method. *Pharm. Res.* **14**:128–134 (1997).
13. L. K. Paalzow. Measurement and modeling analgesic drug effect. In C. J. van Boxtel, N. H. G. Holford, and M. Danhof (eds), The *in vivo study of drug action—Principles and applications of kinetic-dynamic modelling,* Elsevier Science Publishers B.V., Amsterdam, 1992, pp. 133–153.
14. M. R. Bouw and M. Hammarlund-Udenaes. Methodological aspects of the use of a calibrator in in vivo microdialysis—further development of the retrodialysis method. *Pharm. Res.* **15**:1673–1679 (1998).
15. M. N. Carroll and R. K. S. Lim. Observation on the neuropharmacology of morphine and morphinelike analgesia. *Arch. Int. Pharmacodyn. Ther.* **125**:383–403 (1960).
16. M. Ekblom, M. Gårdmark, and U. M. Hammarlund. Estimation of unbound concentrations of morphine from microdialysate concentrations by use of nonlinear regression analysis in vivo and in vitro during steady state conditions. *Life Sci.* **51**:449–460 (1992).
17. S. L. Beal and L. S. Sheiner. NONMEM user's guide. NONMEM Project Group, 1992, University of California at San Francisco: San Francisco.
18. E. N. Jonsson and M. O. Karlsson. Xpose—An S-PLUS based population pharmacokinetic/pharmacodynamic model building aid for NONMEM. *Comput. Methods Programs Biomed.* **58**:51–64 (1999).
19. L. B. Sheiner, D. R. Stanski, S. Vozeh, R. D. Miller, and J. Ham. Simultaneous modeling of pharmacokinetics and pharmacody-

namics: Application to d-tubocurarine. *Clin. Pharmacol. Ther.* **25**: 358–371 (1979).
20. G. Skopp, L. Potsch, B. Ganssmann, R. Aderjan, and R. Mattern. A preliminary study on the distribution of morphine and its glucuronides in the subcompartments of blood. *J Anal Toxicol.* **22**: 261–264 (1998).
21. R. Xie, M. Hammarlund-Udenaes, A. G. de Boer, and E. C. de Lange. The role of P-glycoprotein in blood-brain barrier transport of morphine: Transcortical microdialysis studies in mdr1a (-/-) and mdr1a (+/+) mice. *Br. J. Pharmacol.* **128**:563–568 (1999).
22. M. Ekblom, M. Hammarlund-Udenaes, and L. K. Paalzow. Modeling of tolerance development and rebound effect during different intravenous administrations of morphine to rats. *J. Pharmacol. Exp. Ther.* **266**:244–252 (1993).
23. D. M. Ouellet and G. M. Pollack. Pharmacodynamics and tolerance development during multiple intravenous bolus morphine administration in rats. *J. Pharmacol. Exp. Ther.* **281**:713–720 (1997).
24. D. M. Ouellet and G. M. Pollack. Effect of prior morphine-3-glucuronide exposure on morphine disposition and antinociception. *Biochem Pharmacol.* **53**:1451–1457 (1997).
25. S. P. Letrent, G. M. Pollack, K. R. Brouwer, and K. L. Brouwer. Effect of GF120918, a potent P-glycoprotein inhibitor, on morphine pharmacokinetics and pharmacodynamics in the rat. *Pharm. Res.* **15**: 599–605 (1998).
26. M. Gårdmark, A. U. Höglund, and M. Hammarlund-Udenaes. Aspects on tail-flick, hot-plate and electrical stimulation tests for morphine antinociception. *Pharmacol. Toxicol.* **83**:252–258 (1998).
27. S. P. Letrent, G. M. Pollack, K. R. Brouwer, and K. L. Brouwer. Effects of a potent and specific P-glycoprotein inhibitor on the blood-brain barrier distribution and antinociceptive effect of morphine in the rat. *Drug. Metab. Dispos.* **27**:827–834 (1999).
28. F. Stain, M. J. Barjavel, P. Sandouk, M. Plotkine, J. M. Scherrmann, and H. N. Bhargava. Analgesic response and plasma and brain extracellular fluid pharmacokinetics of morphine and morphine-6-beta-D-glucuronide in the rat. *J. Pharmacol. Exp. Ther.* **274**(2): 852–857 (1995).
29. Y. Wang and R. J. Sawchuk. Zidovudine transport in the rabbit brain during intravenous and intracerebroventricular infusion. *J. Pharm. Sci.* **84**:871–876 (1995).
30. C. K. Kuo, N. Hanioka, Y. Hoshikawa, K. Oguri, and H. Yoshimura. Species difference of site-selective glucuronidation of morphine. *J. Pharmacobio-Dyn.* **14**:187–193 (1991).
31. M. Ekblom, M. Gårdmark, and M. Hammarlund-Udenaes. Pharmacokinetics and pharmacodynamics of morphine-3-glucuronide in rats and its influence on the antinociceptive effect of morphine. *Biopharm. Drug Disp.* **14**:1–11 (1993).
32. M. Gårdmark, M. O. Karlsson, F. Jonsson, and M. Hammarlund-Udenaes. Morphine-3-glucuronide has a minor effect on morphine antinociception. Pharmacodynamic modeling. *J. Pharm. Sci.* **87**:813–820 (1998).